4 (2025) 100258

Contents lists available at ScienceDirect

Journal of Subatomic Particles and Cosmology

journal homepage: https://www.sciencedirect.com/journal/journal-of-subatomic-particles-and-cosmology

Approaching the continuum with anisotropic lattice thermodynamics

Jon-Ivar Skullerud [a,b,*], Gert Aarts [c], Chris Allton [c], M. Naeem Anwar [c], Ryan Bignell [b], Tim Burns [c], Simon Hands [d], Rachel Horohan D'Arcy [a], Ben Jäger [e], Seyong Kim [f], Alan Kirby [c], Maria Paola Lombardo [g], Seung-Il Nam [h], Sinéad M. Ryan [b], Antonio Smecca [c]

[a] Department of Physics, Maynooth University—National University of Maynooth, Maynooth, Ireland
[b] School of Mathematics, Trinity College, Dublin, Ireland
[c] Centre for Quantum Fields and Gravity, Department of Physics, Swansea University, Singleton Park, Swansea, UK
[d] Department of Mathematical Sciences, University of Liverpool, Liverpool, UK
[e] Quantum Field Theory Center & Danish IAS, Department of Mathematics and Computer Science, University of Southern Denmark, 5230 Odense M, Denmark
[f] Department of Physics, Sejong University, Seoul, 05006, Korea
[g] INFN, Sezione di Firenze, 50019 Sesto Fiorentino, 50019, Italy
[h] Department of Physics, Pukyong National University (PKNU), Busan, 48513, Korea

ARTICLE INFO

Keywords:
Quantum chromodynamics
Lattice QCD
Quark-gluon plasma
Chiral symmetry restoration

ABSTRACT

The FASTSUM collaboration has a long-standing programme of using anisotropic lattice QCD to investigate strong interaction thermodynamics, and in particular spectral quantities. Here we present first results from our new ensemble which has a temporal lattice spacing $a_\tau = 15$ am and anisotropy $\xi = a_s/a_\tau = 7$, giving unprecedented resolution in the temporal direction. We show results for the chiral transition, vector–axial-vector degeneracy, and heavy quarkonium, and compare them with earlier results with coarser time resolution.

1. Introduction

Many of the most interesting, yet poorly determined properties of the quark–gluon plasma (QGP) created in heavy-ion collisions are spectral quantities. These include, firstly, transport properties such as conductivity, diffusion coefficients, and viscosities; and secondly, hadronic properties such as their degeneracy patterns, mass shifts, width, and dissociation in the QGP. Determining such properties from euclidean correlation functions is known to be an ill-posed problem as it involves solving the integral equation

$$G_E(\tau;T) = \int_0^\infty d\omega K(\omega,\tau;T)\rho(\omega;T), \tag{1}$$

where G_E is the euclidean correlator, ρ is the (unknown) spectral function, and K is a known integral kernel. The ill-posed nature of this problem arises from a combination of the limited number of euclidean data points and their statistical uncertainties. In order to mitigate the first of these issues, the FASTSUM collaboration has been using anisotropic lattices, where the temporal resolution is much finer than the spatial one. This has yielded a wealth of information including on heavy quark physics [1–7], electrical conductivity [8,9], and parity doubling in baryons [6,10–12].

The parameters of the ensembles we have used to date are given in Table 1. In these proceedings, we present initial results from our newest "Generation 3" ensemble, where the temporal lattice spacing is about half that of our previous ensembles. This will give us unprecedented temporal resolution and hence assist spectral reconstruction, while also allowing a denser set of temperatures than hitherto possible in the fixed-scale approach. We present our procedure for tuning the parameters in Section 2. In Section 3.1 we present initial results for the chiral transition including the vector–axial-vector degeneracy, while Section 3.2 presents preliminary results for the temperature dependence of heavy quarkonium. We conclude with an overview of planned future work on this and future ensembles.

* Corresponding author.
E-mail addresses: jonivar.skullerud@mu.ie (J.-I. Skullerud), g.aarts@swansea.ac.uk (G. Aarts), C.R.Allton@swansea.ac.uk (C. Allton), m.n.anwar@swansea.ac.uk (M.N. Anwar), bignellr@tcd.ie (R. Bignell), T.Burns@swansea.ac.uk (T. Burns), simon.hands@liverpool.ac.uk (S. Hands), rachel.horohandarcy.2018@mumail.ie (R. Horohan D'Arcy), jaeger@imada.sdu.dk (B. Jäger), skim@sejong.ac.kr (S. Kim), 967741@Swansea.ac.uk (A. Kirby), Mariapaola.Lombardo@lnf.infn.it (M.P. Lombardo), sinam@pknu.ac.kr (S.-I. Nam), ryan@maths.tcd.ie (S.M. Ryan), antonio.smecca@swansea.ac.uk (A. Smecca).

https://doi.org/10.1016/j.jspc.2025.100258
Received 26 September 2025; Accepted 31 October 2025
Available online 10 November 2025

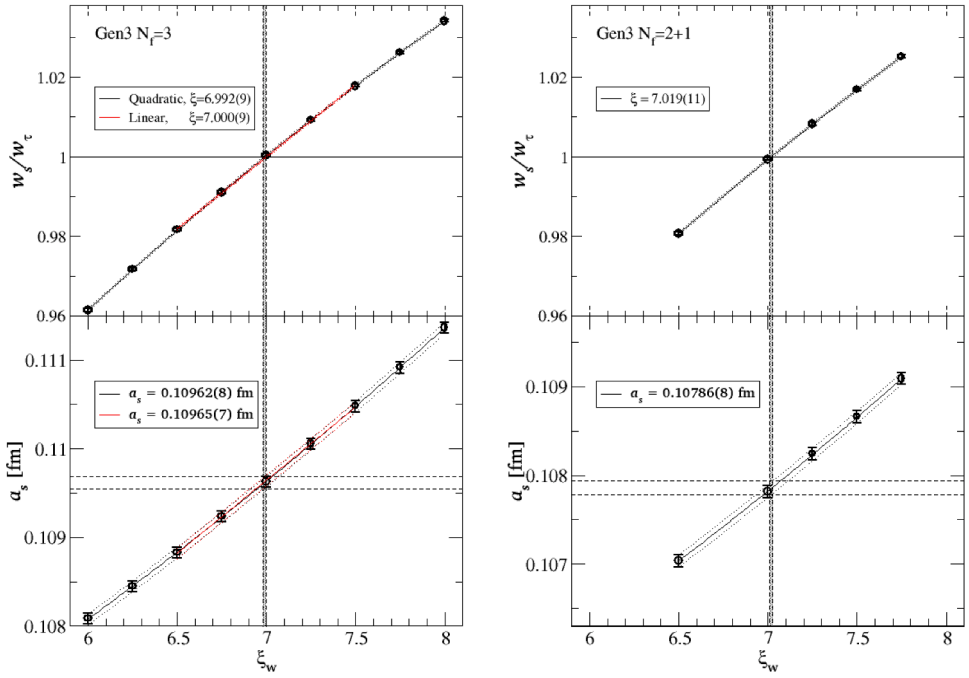

Fig. 1. Gauge anisotropy (top) and lattice spacing (bottom) from the Wilson flow. Left: $N_f = 3$, including linear and quadratic fits. Right: $N_f = 2+1$, including quadratic fits.

Table 1
FASTSUM ensembles: ensemble label (Generation), number of quark flavours N_f, spatial and temporal lattice spacings a_s, a_τ and anisotropy $\xi = a_s/a_\tau$, pion mass m_π and spatial extent $L_s = a_s N_s$.

Gen	N_f	ξ	a_s (fm)	a_τ^{-1} (GeV)	m_π (MeV)	N_s	L_s (fm)
1	2	6.0	0.162(4)	7.35(3)	490	12	1.94
2	2+1	3.45	0.1205(8)	5.63(4)	384(4)	24	2.95
						32	3.94
2L	2+1	3.45	0.1121(3)	6.08(1)	239(1)	32	3.58
3	2+1	7.0	0.108(1)	12.82(7)	378(1)	32	3.49

2. Tuning the action parameters

Our simulations are carried out using anisotropic lattices with an $\mathcal{O}(a^2)$ improved gauge action and an $\mathcal{O}(a)$ improved Wilson fermion action with stout smearing, following the approach of the HadSpec collaboration [13,14], who carried out the tuning for our Gen2 and Gen2L ensembles. The details of the action are given in [15]. It contains four independent parameters: the gauge coupling β, the bare gauge and fermion anisotropies γ_g, γ_f, and the bare quark mass m_0. These must be tuned simultaneously to obtain the desired values for the quantities a_s, ξ_g, ξ_f, m_π, where ξ_g and ξ_f are measured anisotropies in the gauge and fermion sector respectively.

We have carried out the parameter tuning at the 3-flavour symmetric point, with the target values

$$a_s \approx a_s(\text{Gen2}) = 0.12\,\text{fm}, \qquad \xi_g = \xi_f = 7.0, \qquad \frac{m_{PS}^{3\text{fl}}}{m_V^{3\text{fl}}} = 0.545, \tag{2}$$

where the last value is obtained from the 3-flavour symmetric equivalent of the Gen2 values,

$$\frac{1}{3}\left(\frac{m_{PS}^{3\text{fl}}}{m_V^{3\text{fl}}}\right)^2 = \frac{m_\pi^2 + 2m_K^2}{(m_\rho + 2m_{K^*})^2}\Big|_{\text{Gen2}}. \tag{3}$$

Following this, β, γ_g and γ_q have been fixed and the light and strange bare quark masses tuned to reproduce the Gen2 pion mass, $m_\pi =$ 390 MeV, and the physical value for m_{η_s}/m_ϕ, where $m_{\eta_s} = \sqrt{2m_K^2 - m_\pi^2}$ is the mass of the would-be $s\bar{s}$ pseudoscalar.

2.1. 3-flavour tuning

For the 3-flavour tuning, we have generated ~ 100 ensembles of $N_\tau \times N_s^3 = 256 \times 24^3$ lattices with ~ 2000 molecular dynamics trajectories each.

The gauge anisotropy and (spatial) lattice spacing have been determined using the Symanzik flow method introduced in [16]. For an isotropic lattice, the w_0 scale is defined as where the flowed fields satisfy the condition

$$\left[t\frac{d}{dt}t^2E(t)\right]_{t=w_0^2} = 0.3, \qquad E(t) = \frac{1}{4}\sum_{\mu\nu}F_{\mu\nu}^2, \tag{4}$$

and we take the most recent FLAG [17] value, $w_0 = 0.17355(92)$ fm. In the case of an anisotropic lattice, with $a_s = \xi a_\tau$, we have

$$E_{ij}^{\text{phys}} = a_s^4 E_{ij}^{\text{lat}}, \qquad E_{i4}^{\text{phys}} = a_s^2 a_\tau^2 E_{i4}^{\text{lat}}, \tag{5}$$

and the flow equation now includes the flow anisotropy parameter ξ_w. We may also define the spatial and temporal w-scales, w_s, w_τ:

$$\left[t\frac{d}{dt}t^2E_{ss}(t)\right]_{t=w_s^2} = 0.15, \qquad \xi_w^2\left[t\frac{d}{dt}t^2E_{s\tau}(t)\right]_{t=w_\tau^2} = 0.15\,.$$

The physical gauge anisotropy ξ_g can now be determined as the value for ξ_w where $w_s = w_\tau$, and the lattice spacing is determined from the value of $w_s = w_\tau = w_0$ at this flow anisotropy. Fig. 1 illustrates this for our final 3-flavour symmetric ensemble as well as for the 2+1 flavour ensemble. We see that the anisotropy and lattice spacing are both almost unchanged when going from $N_f = 3$ to $N_f = 2+1$ at fixed $\beta, \gamma_g, \gamma_f$.

The fermion anisotropy is determined from the pseudoscalar and vector meson dispersion relations, as shown in Fig. 2. From the 3-flavour symmetric dispersion relations in the left panel, we see that the resulting anisotropies agree very well both with each other and with the target (and gauge) anisotropy of 7.0. The spatial lattice spacing comes out slightly smaller than for the Gen2 ensemble, which should be taken into account when comparing results from the two.

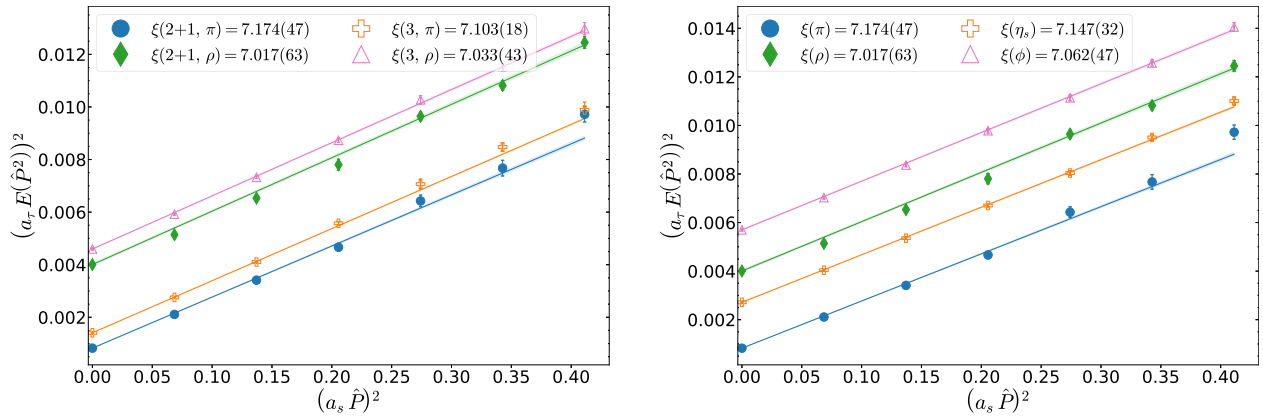

Fig. 2. Left: light pseudoscalar and vector dispersion relation for the $N_f = 3$ and $N_f = 2+1$ ensembles. Right: Light and strange meson dispersion relations for the $N_f = 2+1$ ensemble. Note that the blue circles and green diamonds are the same in both plots. (For interpretation of the references to colour in this figure legend, the reader is referred to the web version of this article.)

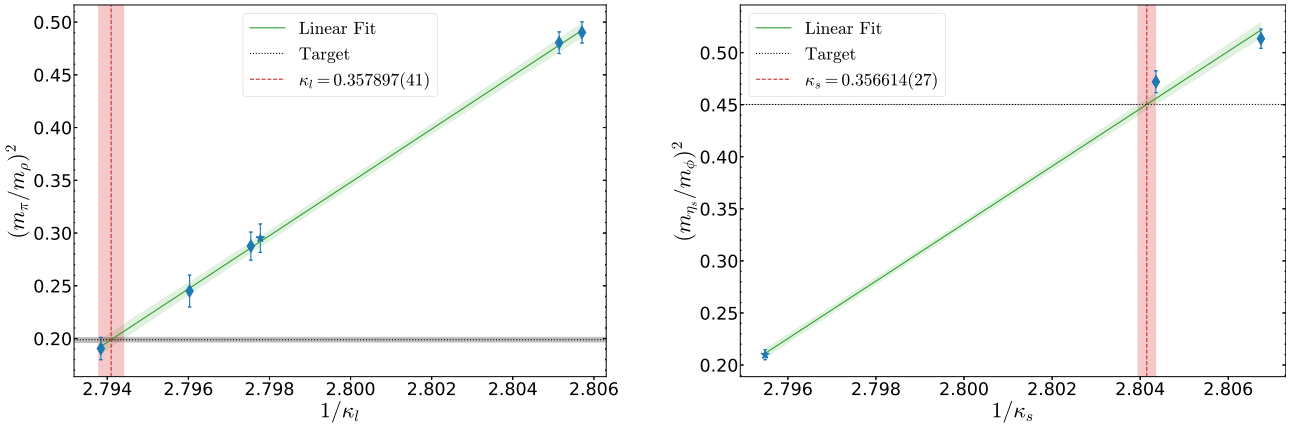

Fig. 3. Left: The squared pseudoscalar-to-vector meson mass ratio as a function of the bare quark mass (inverse hopping parameter), for a number of valence quark masses on the 3-flavour ensemble. Right: The strange pseudoscalar-to-vector mass ratio on an $N_f = 2+1$ background.

2.2. 2+1 flavour tuning

Following the 3-flavour tuning, the light quark mass was determined by producing correlators with various valence quark masses on the 3-flavour ensemble, as shown in Fig. 3 (left). This produced estimates for the light and strange bare quark masses which were used to generate $N_f = 2+1$ ensembles, and the procedure was iterated to yield the final mass parameters. The strange quark mass was tuned by requiring that the dimensionless ratio m_{η_s}/m_ϕ takes on its physical value, as shown in Fig. 3 (right). We have confirmed that different methods to fix the strange quark mass give consistent results.

Finally, the lattice spacing and gauge and fermion anisotropies were determined using the same procedures as in Section 2.1, as shown in the right panels of Figs. 1 and 2. This yields results consistent with those from the 3-flavour ensembles, with the lattice spacing slightly reduced. Furthermore, we find that the Ω^- mass comes out close to its physical value, or conversely, that setting the scale from the Ω^- mass gives results consistent with the w_0 scale setting.

3. Results

Using our $N_f = 2+1$ parameters from the tuning process, we have generated gauge configurations at 14 temperatures ranging from 100 to 530 MeV, in addition to our zero-temperature (256×24^3) ensemble. At each temperature we have generated approximately 1000 configurations separated by 10 MD trajectories. In the following we present some preliminary results from these ensembles.

3.1. Chiral transition

First we consider the standard order parameter of the chiral transition, the chiral condensate $\langle\bar{\psi}\psi\rangle$, and its derivative, the chiral susceptibility $\chi_{\bar{\psi}\psi}$. In the fixed-scale approach, the (additive and multiplicative) renormalisation is temperature-independent, so for the purposes of determining the chiral transition temperature it is sufficient to consider unrenormalised (but vacuum subtracted) quantities, which is what we will do here.

In Fig. 4 we show the bare, vacuum subtracted chiral condensate $\Delta_{\bar{\psi}\psi} = \langle\bar{\psi}\psi\rangle - \langle\bar{\psi}\psi\rangle_0$ and susceptibility $\Delta_\chi = \chi_{\bar{\psi}\psi} - \chi_{\bar{\psi}\psi,0}$. These quantities have been made dimensionless by dividing by appropriate powers of the Ω^- mass. The pseudocritical temperature is given by the inflection point in $\Delta_{\bar{\psi}\psi}$ or the peak in Δ_χ; we determine this by fitting the data to functions given by

$$\Delta_{\bar{\psi}\psi} = c_1 + c_2 \arctan\left[c_2(T - T_c^{\bar{\psi}\psi})\right]; \qquad \Delta_\chi = c_2 + \frac{c_0}{c_1 + (T - T_c^\chi)^2}. \tag{6}$$

This gives us $T_c^{\bar{\psi}\psi} \sim 182$ MeV and $T_c^\chi \sim 178$ MeV (a full error analysis is in progress). These values are very close to those of the Gen2 ensemble (also shown in Fig. 4), which has the same pion mass and a similar (but slightly larger) spatial lattice spacing, suggesting that reducing the temporal lattice spacing alone does not have a big effect on the location of the chiral transition.

Another signal of restoration of chiral symmetry is that the vector and axial-vector meson correlators become degenerate. Following [18], we introduce the correlator ratio $R_{VA}(\tau)$ and the summed ratio R_{VA} as

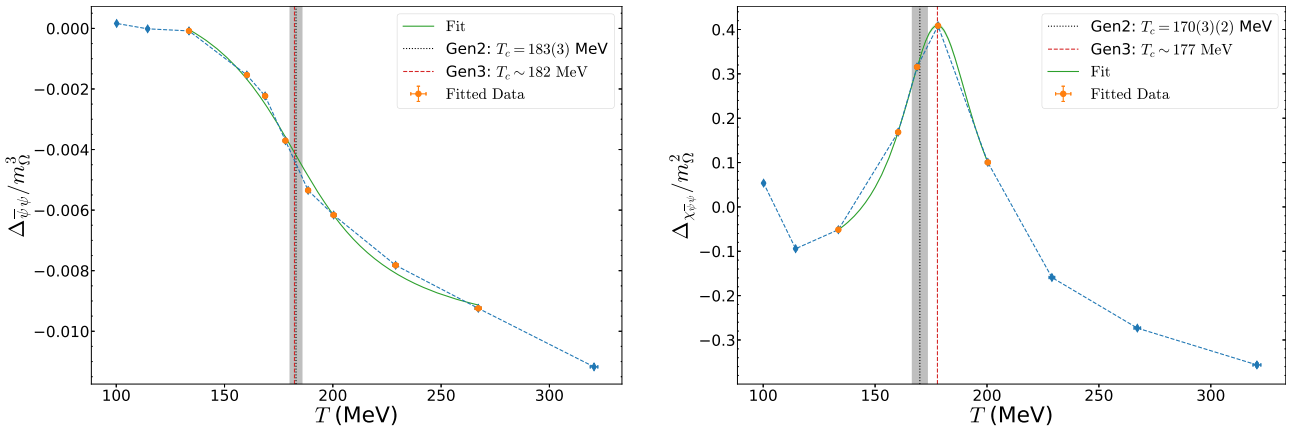

Fig. 4. Left: The dimensionless bare subtracted chiral condensate. Right: The dimensionless chiral susceptibility. The dashed lines are there to guide the eye, while the continuous lines are fits to (6), using the data points represented by the orange diamonds.

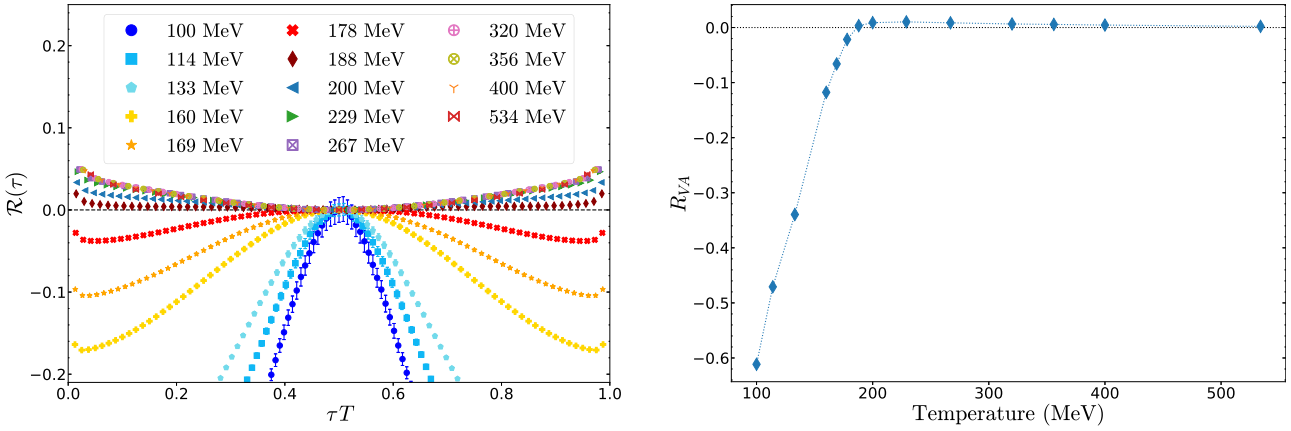

Fig. 5. Left: The $V-A$ degeneracy ratio $\mathcal{R}_{VA}(\tau)$ for all temperatures. Right: The summed degeneracy ratio $\mathcal{R}_{VA}$ as a function of temperature.

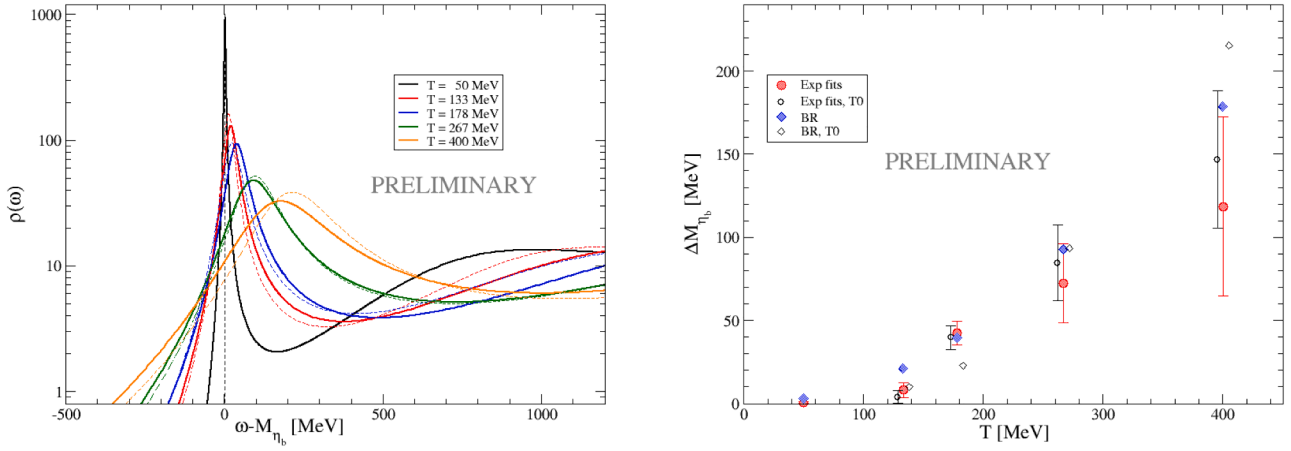

Fig. 6. Left: η_b spectral functions from the BR method at different temperatures. The solid lines are obtained from the thermal ensembles, while the dashed lines are obtained from the $T = 0$ ensembles using the same temporal range (see text). Right: Mass of the η_b meson minus its zero-temperature value, from exponential fits and from the BR method. The filled points are results from the thermal ensembles, while the open symbols are from the $T = 0$ analysis with the same temporal range.

measures of this degeneracy:

$$\mathcal{R}_{VA}(\tau) = \frac{G_A(\tau) - G_V(\tau)}{G_A(\tau) + G_V(\tau)}, \qquad \mathcal{R}_{VA} = \frac{\sum_{n=n_{\min}}^{N_\tau/2-1} \mathcal{R}_{VA}(\tau_n)/\sigma^2(\tau_n)}{\sum_{n=n_{\min}}^{N_\tau/2-1} 1/\sigma^2(\tau_n)} \tag{7}$$

These are shown in Fig. 5, using smeared correlators normalised at $\tau = N_\tau/2$, and taking $n_{\min} = 7$. Since Wilson fermions explicitly break chiral symmetry, $\mathcal{R}_{VA}(\tau)$ will deviate from zero at small τ even at high temperature; however, in Fig. 5 we clearly see that the vector and axial-vector correlators become approximately degenerate above $T \sim 180 - 200$ MeV, consistent with the pseudocritical temperature determined from the chiral condensate. The pattern is in agreement with that previously found for the Gen2 and Gen2L ensembles [18].

3.2. Heavy quarkonium

We have simulated beauty quarks on our Gen3 ensemble with a nonrelativistic QCD (NRQCD) hamiltonian including $\mathcal{O}(v^4)$ terms. The quark mass was tuned using the dispersion relation for the η_b and Υ states,

$$E(\vec{p}) = E_0 + \frac{p^2}{2\bar{M}}, \tag{8}$$

such that the kinetic mass $\bar{M}$ equals the spin-averaged 1S mass, $\bar{M} = (m_{\eta_b} + 3m_\Upsilon)/4$.

Preliminary results for the pseudoscalar (η_b) state using exponential correlator fits and spectral function reconstruction using the BR method [19] are shown in Fig. 6. In addition to the thermal correlators, we have performed the same analysis on zero-temperature correlators with the temporal extent limited to $\tau \in (0, 1/T)$ for each temperature T. This will assist in disentangling true thermal effects from those arising merely from restricting the temporal range in the analysis. Within the current uncertainties, these preliminary results suggest that the apparent mass shift is entirely due to restricting the temporal range and hence not physical, but at the present level, a small thermal mass shift as observed in the Gen2L analysis [7,20] is not yet ruled out.

4. Outlook

We have presented the first results from the new "Gen3" ensemble of anisotropic lattices with a temporal lattice spacing $a_\tau = 15.5$ am, which is half that of our previous ensembles. This is an important step towards controlling lattice spacing effects in our simulations, and will give improved control in extracting spectral quantities. We have shown preliminary results for the chiral transition including a clear signal of degeneracy between the vector and axial-vector channels, as well as for the bottomonium mass and spectral function. Work on other quantities including light mesons and baryons and charm physics is underway.

We are also working on tuning parameters for two new ensembles: Gen2P, which will have roughly the same anisotropy and lattice spacing as Gen2 and Gen2L, but with physical light quarks ($m_\pi = 140$ MeV), and Gen3L, which will have the same parameters as Gen3 but with a pion mass $m_\pi = 240$ MeV. We expect production of these ensembles to start shortly, and hence provide further control of the systematics in our calculations.

CRediT authorship contribution statement

Jon-Ivar Skullerud: Conceptualization, Formal analysis, Investigation, Methodology, Project administration, Software, Supervision, Writing – original draft, Writing – review & editing; **Gert Aarts:** Writing – review & editing, Funding acquisition, Conceptualization; **Chris Allton:** Conceptualization, Funding acquisition, Methodology, Project administration, Resources, Supervision, Writing – review & editing; **M. Naeem Anwar:** Writing – review & editing; **Ryan Bignell:** Data curation, Formal analysis, Investigation, Methodology, Software, Validation, Visualization, Writing – review & editing; **Tim Burns:** Methodology, Supervision, Writing – review & editing; **Simon Hands:** Funding acquisition, Supervision; **Rachel Horohan D'Arcy:** Investigation, Methodology, Software; **Ben Jäger:** Investigation, Resources, Software, Validation; **Seyong Kim:** Conceptualization, Funding acquisition, Methodology, Resources, Software, Writing – review & editing; **Alan Kirby:** Software; **Maria Paola Lombardo:** Conceptualization, Writing – review & editing; **Seung-Il Nam:** Conceptualization, Methodology; **Sinéad M. Ryan:** Funding acquisition, Methodology, Supervision, Writing – review & editing; **Antonio Smecca:** Conceptualization, Formal analysis, Investigation, Methodology, Software, Validation, Writing – review & editing.

Data availability

Data will be made available in a forthcoming publication when the analysis is completed

Declaration of interests

The authors declare the following financial interests/personal relationships which may be considered as potential competing interests: M. Naeem Anwar reports financial support was provided by The Royal Society. Gert Aarts, Chris Allton, Ryan Bignell, Timothy Burns, Antonio Smecca reports financial support was provided by Science and Technology Facilities Council. Ryan Bignell, Sinead Ryan reports financial support was provided by Research Ireland. All authors reports equipment, drugs, or supplies was provided by Science and Technology Facilities Council DiRAC. All authors reports equipment, drugs, or supplies was provided by European High Performance Computing Joint Undertaking. Jon-Ivar Skullerud reports equipment, drugs, or supplies was provided by Irish Centre for High-End Computing. All authors reports equipment, drugs, or supplies was provided by Supercomputing Wales. All authors reports equipment, drugs, or supplies was provided by Partnership for Advanced Computing In Europe. If there are other authors, they declare that they have no known competing financial interests or personal relationships that could have appeared to influence the work reported in this paper.

Acknowledgment

We thank Aoife Kelly for her contribution in the early stages of this work. G.A., C.A., R.B., T.J.B. and A.S. are grateful for support via STFC grants ST/T000813/1 and ST/X000648/1. M.N.A. acknowledges support from The Royal Society Newton International Fellowship. R.B. and S.M.R. acknowledge support from a Science Foundation Ireland Frontiers for the Future Project award with grant number SFI-21/FFP-P/10186. This work used the DiRAC Extreme Scaling service at the University of Edinburgh, operated by the Edinburgh Parallel Computing Centre and the DiRAC Data Intensive service operated by the University of Leicester IT Services on behalf of the STFC DiRAC HPC Facility https://www.dirac.ac.uk. This equipment was funded by BEIS capital funding via STFC capital grants ST/R00238X/1, ST/K000373/1 and ST/R002363/1 and STFC DiRAC Operations grants ST/R001006/1 and ST/R001014/1. DiRAC is part of the UK National e-Infrastructure. We acknowledge the support of the Swansea Academy for Advanced Computing, the Supercomputing Wales project, which is part-funded bythe European Regional Development Fund (ERDF) via Welsh Government, and the University of Southern Denmark and ICHEC, Ireland for use of computing facilities. This work was performed using PRACE resources at Cineca (Italy), CEA (France) and Stuttgart (Germany) via grants 2015133079, 2018194714, 2019214714 and 2020214714. We acknowledge EuroHPC Joint Undertaking for awarding the project EHPC-EXT-2023E01-010 access to LUMI-C, Finland.

References

[1] G. Aarts, C. Allton, M.B. Oktay, M. Peardon, J.-I. Skullerud, Charmonium at high temperature in two-flavor QCD, Phys. Rev. D 76 (2007) 94513. arXiv:0705.2198. https://doi.org/10.1103/PhysRevD.76.094513

[2] G. Aarts, C. Allton, S. Kim, M.P. Lombardo, M.B. Oktay, et al., What happens to the Υ and η_b in the quark-gluon plasma? Bottomonium spectral functions from lattice QCD, JHEP 1111 (2011) 103. arXiv:1109.4496. https://doi.org/10.1007/JHEP11(2011)103

[3] G. Aarts, C. Allton, T. Harris, S. Kim, M.P. Lombardo, et al., The bottomonium spectrum at finite temperature from $N\_f = 2 + 1$ lattice QCD, JHEP 1407 (2014) 97. arXiv:1402.6210. https://doi.org/10.1007/JHEP07(2014)097

[4] A. Kelly, A. Rothkopf, J.-I. Skullerud, Bayesian study of relativistic open and hidden charm in anisotropic lattice QCD, Phys. Rev. D 97 (11) (2018) 114509. arXiv:1802.00667. https://doi.org/10.1103/PhysRevD.97.114509

[5] G. Aarts, C. Allton, R. Bignell, T.J. Burns, S.C.G. á Mascaraque, S. Hands, B. Jäger, S. Kim, S.M. Ryan, J.-I. Skullerud, Open charm mesons at nonzero temperature: results in the hadronic phase from lattice QCD, 2022. arXiv:2209.14681

[6] G. Aarts, C. Allton, M.N. Anwar, R. Bignell, T.J. Burns, B. Jäger, J.-I. Skullerud, Non-zero temperature study of spin 1/2 charmed baryons using lattice gauge theory, Eur. Phys. J. A 60 (3) (2024) 59. arXiv:2308.12207. https://doi.org/10.1140/epja/s10050-024-01261-2

[7] J.-I. Skullerud, et al., Spectral properties of bottomonium at high temperature: a systematic investigation, in: 16th Conference on Quark Confinement and the Hadron Spectrum, Proc. Sci. QCHSC24 2025 160. arXiv:2503.17315. https://doi.org/10.22323/1.483.0160.

[8] A. Amato, G. Aarts, C. Allton, P. Giudice, S. Hands, J.-I. Skullerud, Electrical conductivity of the quark-gluon plasma across the deconfinement transition, Phys.Rev.Lett. 111 (2013) 172001. arXiv:1307.6763. https://doi.org/10.1103/PhysRevLett.111.172001

[9] G. Aarts, C. Allton, A. Amato, P. Giudice, S. Hands, J.-I. Skullerud, Electrical conductivity and charge diffusion in thermal QCD from the lattice, JHEP 1502 (2015) 186. arXiv:1412.6411. https://doi.org/10.1007/JHEP02(2015)186

[10] G. Aarts, C. Allton, S. Hands, B. Jäger, C. Praki, J.-I. Skullerud, Nucleons and parity doubling across the deconfinement transition, Phys. Rev. D 92 (1) (2015) 14503. arXiv:1502.03603. https://doi.org/10.1103/PhysRevD.92.014503

[11] G. Aarts, C. Allton, D. de Boni, S. Hands, B. Jäger, C. Praki, J.-I. Skullerud, Light baryons below and above the deconfinement transition: medium effects and parity doubling, JHEP (06) (2017) 34. arXiv:1703.09246. https://doi.org/10.1007/JHEP06(2017)034

[12] G. Aarts, C. Allton, D. de Boni, B. Jäger, Hyperons in thermal QCD: a lattice view, Phys. Rev. D 99 (7) (2019) 74503. arXiv:1812.07393. https://doi.org/10.1103/PhysRevD.99.074503

[13] R.G. Edwards, B. Joó, H.-W. Lin, Tuning for three-flavors of anisotropic clover fermions with stout-link smearing, Phys.Rev. D 78 (2008) 54501. arXiv:0803.3960. https://doi.org/10.1103/PhysRevD.78.054501

[14] H.-W. Lin, et al., First results from $2+1$ dynamical quark flavors on an anisotropic lattice: Light-Hadron spectroscopy and setting the strange-quark mass, Phys.Rev. D 79 (2009) 34502. arXiv:0810.3588. https://doi.org/10.1103/PhysRevD.79.034502

[15] G. Aarts, et al., Properties of the QCD thermal transition with $N_f = 2+1$ flavours of Wilson quark, Phys. Rev. D 105 (3) (2022) 34504. arXiv:2007.04188. https://doi.org/10.1103/PhysRevD.105.034504

[16] S. Borsányi, S. Dürr, Z. Fodor, S. Katz, S. Krieg, et al., Anisotropy tuning with the Wilson flow, (2012).arXiv:1205.0781.

[17] Y. Aoki, et al., FLAG Review 2024 (2024). arXiv:2411.04268.

[18] A. Smecca, G. Aarts, C. Allton, R. Bignell, B. Jäger, S.I. Nam, S. Kim, J.-I. Skullerud, L.-K. Wu, The curvature of the pseudo-critical line in the QCD phase diagram from mesonic lattice correlation functions, (2024). arXiv:2412.20922.

[19] Y. Burnier, A. Rothkopf, Bayesian approach to spectral function reconstruction for euclidean quantum field theories, Phys. Rev. Lett. 111 (2013) 182003. arXiv:1307.6106. https://doi.org/10.1103/PhysRevLett.111.182003

[20] M.P. Lombardo, et al., Bottomonium spectral functions in thermal QCD, J. Subatomic Part. Cosmol 3 (2025) 100049. https://doi.org/10.1016/j.jspc.2025.100049